



저작자표시-비영리-변경금지 2.0 대한민국

이용자는 아래의 조건을 따르는 경우에 한하여 자유롭게

- 이 저작물을 복제, 배포, 전송, 전시, 공연 및 방송할 수 있습니다.

다음과 같은 조건을 따라야 합니다:



저작자표시. 귀하는 원저작자를 표시하여야 합니다.



비영리. 귀하는 이 저작물을 영리 목적으로 이용할 수 없습니다.



변경금지. 귀하는 이 저작물을 개작, 변형 또는 가공할 수 없습니다.

- 귀하는, 이 저작물의 재이용이나 배포의 경우, 이 저작물에 적용된 이용허락조건을 명확하게 나타내어야 합니다.
- 저작권자로부터 별도의 허가를 받으면 이러한 조건들은 적용되지 않습니다.

저작권법에 따른 이용자의 권리는 위의 내용에 의하여 영향을 받지 않습니다.

이것은 [이용허락규약\(Legal Code\)](#)을 이해하기 쉽게 요약한 것입니다.

[Disclaimer](#)

Master's Thesis

**Development of *in vivo*
microbial tracking system using
streptavidin-expressing
bacteria**

Department of Biomedical Science
Graduate School, Chonnam National University

Jin Hee Im

August 2022

Development of *in vivo* microbial tracking system using streptavidin-expressing bacteria

Department of Biomedical Science
Graduate School, Chonnam National University

Jin Hee Im

Supervised by Professor Seong Young Kwon

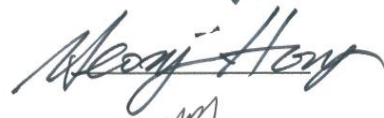
A dissertation submitted in partial fulfillment of the requirements
for the Master of Biomedical Science

Committee in Charge :

Jung-Joon Min



Yeongjin Hong



Seong Young Kwon



August 2022

TABLE OF CONTENTS

TABLE OF CONTENTS.....	I
LIST OF FIGURES.....	II
(ABSTRACT).....	1
I. INTRODUCTION.....	3
II. MATERIALS AND METHODS.....	5
A. Bacterial culture.....	5
B. Construction of expression plasmids for mSA fused with maltose-binding protein (MBP) and Ribosome binding site (RBS).....	5
C. Western blot analysis.....	6
D. Bacterial uptake assay of biotinylated dye.....	7
E. <i>In vivo</i> fluorescent imaging in mice	8
F. Bacterial counting and mSA expression	8
G. Statistical analysis.....	9
III. RESULTS.....	10
A. Plasmid engineering for mSA expression optimization.....	10
B. Comparison of mSA expression and biotin binding activity	10
C. <i>In vivo</i> imaging.....	11
D. Bacterial counts and mSA expression in liver and intestine tissues.....	12
IV. DISCUSSION.....	22
REFERENCES.....	26
(국문 초록).....	28

LIST OF FIGURES

Figure 1. A schematic diagram using RBS library.

Figure 2. Confirmation of mSA expression in regulatory genes constructed according to RBS libraries.

Figure 3. Engineered plasmid structure.

Figure 4. Evaluation of mSA expression.

Figure 5. Biotinylated fluorescent dye uptake test.

Figure 6. Optical fluorescence imaging to check bacteria tracking.

Figure 7. Evaluation of the number of bacteria, mSA expression and biotin binding activity in mice organs.

Figure S1. Construction of vectors, restriction enzymes, and plasmids used in the study.

Table S1. List of primer used in the study

Development of *in vivo* microbial tracking system using streptavidin-expressing bacteria

Jin Hee Im

Department of Biomedical Science
Graduate School, Chonnam National University
(Supervised by Professor Seong Young Kwon)

(Abstract)

We aimed to develop a novel imaging system for *in vivo* bacterial tracking using bacteria expressing streptavidin which binds specifically to biotin. To enhance bacterial expression level and solubility of streptavidin, we constructed the expression plasmid for monomeric streptavidin-rhizavidin recombinant (mSA) gene fused with maltose-binding protein (MBP) protein. Ribosome binding site (RBS) sequence was selected from its library and added to recombinant gene to get the efficient expression. *E. coli* MG1655 was transformed with the recombinant plasmid driven by pBAD promoter (pBAD-RBS-MBP-mSA).

Bacteria were orally administered to mice. The expression of mSA was induced using L-arabinose immediately or 1 hour after bacterial administration. One hour after L-arabinose induction, a biotinylated fluorescent dye was intravenously injected to obtain optical images of bacteria. Optical signals were observed only in

the intestines of mice with L-arabinose induction but not in those with fluorescent dye injection only or without L-arabinose induction after bacterial administration. In *ex vivo* imaging of the intestine, signal was stronger in the mice with immediate L-arabinose induction than in those with induction 1 hour after bacterial administration. The number of bacteria in the intestine was similar among both of mice regardless of L-arabinose induction times. Western blot analysis showed that the expression of mSA and its biotin binding were observed only in intestines with L-arabinose induction.

Taken together, we developed novel tracking system to visualize bacterial distribution *in vivo* using streptavidin and biotin interaction. This system could be applied for real time monitoring of microbial distribution *in vivo* using a various kind of biotinylated imaging probes.

I. INTRODUCTION

Imaging-based bacterial monitoring systems have been developed using several imaging techniques. For optical imaging applications, bacteria were engineered to be transformed with plasmids containing genes of bioluminescent or fluorescent proteins [1, 2]. Although these optical imaging systems are highly efficient for bacteria localization *in vivo*, the poor penetration of signals through tissues limits their usefulness in large animals and clinical applications. Several studies reported that bacteria were directly labeled with diagnostic radionuclides [3]. However, radionuclide-binding bacteria could be diluted after systemic circulation, which reduced *in vivo* imaging signals [4]. Therefore, a new approach is needed to improve *in vivo* detection performance of bacteria for large animals or human.

The usage of imaging molecules specifically bound to proteins expressed in bacteria have the potential to overcome the detection sensitivity of bacteria expressing imaging system. Streptavidin, a tetrameric protein from *Streptomyces avidinii*, was being applied for various biological fields using high binding affinity with biotin [5, 6]. However, the oligomerization of this protein was essential for stability and function but induced inclusion body, resulting in functional changes [7-9]. Also, streptavidin gene fused with other proteins was difficult to be functional because of conformational perturbation by tetramer structure [10]. To overcome these problems, many monomeric forms have been developed and reported [11, 12].

Rizavidin is a streptavidin homolog from the bacterium *Rhizobium etli* and forms a

natural dimer because it has a short loop 7, 8 (L7, 8) and several interfacial mutations that interfere with tetramerization [10]. Especially, the sharing of binding site residues between the subunits is not a prerequisite for stable biotin association and high biotin affinity can be achieved using the residues of a single subunit. In previous study monomeric streptavidin-rhizavidin recombinant (mSA) could achieve optimized biophysical properties by replacing the binding site residues of streptavidin monomer with corresponding rhizavidin residues [7].

In this study, we constructed the bacterial expression plasmid for a mSA fused with specific genes capable of enhancing the expression and solubility. And we also developed a novel imaging system for bacterial tracking *in vivo* using streptavidin-biotin binding interaction.

II. MATERIALS AND METHODS

A. Bacterial culture

E. coli DH5 α was obtained from Enzynomics, Korea and used for plasmid cloning. *E. coli* MG1655 was a gift from Dr. Hyon E Choy, Department of Microbiology, Chonnam National University and used as model bacterium in this study.

All bacteria were *in vitro* cultured at 37 °C with 200 rpm agitation in Luria–Bertani (LB) media. Resulting plasmid, which contained an ampicillin resistance gene, was transformed into competent cell (*E. coli* DH5 α) by electroporati (1.8 kV; Bio–Rad, CA, USA). They were chemically transformed with plasmids as described and selected as appeared colonies on LB agar plate containing ampicillin (100 μ g/ml) after overnight culture. *E. coli* MG1655 was transformed with pBAD–based plasmids. Briefly, bacteria cultured overnight were inoculated in fresh media containing ampicillin as 100–fold dilution. When bacteria reached 0.5–0.7 of optical density at 600 nm (OD₆₀₀), L-arabinose was added to be 0.1% concentration and further cultured.

B. Construction of expression plasmids for mSA fused with maltose–binding protein (MBP) and ribosome binding site (RBS)

Based upon mSA gene sequence [7], pelB–mSA–6xHis gene (mSA with N-terminal pelB leader and C-terminal 6xHis tag) was chemically synthesized (Macrogen, Korea). The synthetic fragment was digested with restriction enzymes NcoI and Sall, cloned into the same sites of pBAD24 plasmid (Fig.S1), and named

pBAD-mSA.

To construct MBP (maltose-binding protein)-mSA fusion gene, mSA fragment with 6xHis tag was amplified with primers, pMAL-mSA_F and pMAL-mSA_R in PCR, digested with EcoRI and HindIII and cloned into EcoRI and HindIII sites of pMAL-MBP. The resulting plasmid was named pMAL-MBP-mSA.

The mSA fragment with C-terminal 6xHis tag was amplified with pBAD-mSA_F and pBAD-mSA_R primers against, in polymerase chain reaction (PCR) and digested with EcoRI and Sall. The digested fragment was cloned into the same sites of pBAD-RBS (Ribosome binding site), and named pBAD-RBS-mSA. MBP-mSA fragment with 6xHis tag was amplified with primers, p2X-mSA_F and mSA_R against pMAL-MBP-mSA as template in PCR and digested with NheI and Sall. The digested fragment was cloned into the same sites of pBAD-RBS, and named pBAD-RBS-MBP-mSA. To highly express protein, optimal RBS against its open reading frame (ORF) was speculated using RBS library calculator program (Penn State University, USA). Specific RBS sequence among the RBS candidates with good translation initiation rate (TIR) was chemically synthesized (Fig. 1). Information on each plasmid and primer is shown in Figure. S1 and Table. S1.

C. Western blot analysis

Three hours after L-arabinose induction, the transformed bacteria were precipitated by centrifugation at 13,000 rpm for 5 minutes. Bacterial pellets (4 OD600 equivalent/well) were dissolved with sodium dodecylsulfate (SDS) sample

buffer containing beta-mercaptoethanol (Sigma-Aldrich, Darmstadt, Germany) and loaded in 12% SDS-polyacrylamide electrophoresis (PAGE). Then, the separated proteins in gel were transferred to a nitrocellulose membrane. The membrane were soaked in Tris-buffered saline with 0.1% Tween 20 (TBS-T) containing 5% skim milk for 2 hour at room temperature. Then, it was incubated with 2,000-fold diluted rabbit anti-His tag antibody (abcam, UK) for overnight. After three-time washing with TBS-T, it was incubated with 5,000-fold horseradish peroxidase conjugated anti-rabbit antibody for 1 hour, visualized by chemiluminescence HRP substrate (Invitrogen, Darmstadt, Germany) and imaged by ChemiDoc™ XRS+ system imager (BIO-RAD, CA, USA). Also, the membrane was incubated with 2000-fold diluted biotinylated peroxidase to measure biotin-binding activity of mSA.

D. Bacterial uptake assay of biotinylated dye

Three hours after L-arabinose induction, the transformed bacteria were incubated with 3.3 ug/ml of biotinylated fluorescent dye (BioActs, Korea) and further cultured. When bacteria reached 3 at OD₆₀₀, they were centrifuged to obtain the pellets and washed with water three times to remove residual dyes in media. Each bacterial sample resuspended in 100 µl water was dispensed into a 96-well black plate (Costar, USA) and its fluorescence level was measured with Infinite m200 fluorescence reader (The spark® multimode microplate reader , Tecan, CA, US). The fluorescence value was measured in excitation at 778 nm and emission at 820 nm.

E. *In vivo* fluorescent imaging in mice

Six-week-old female BALB/c mice (weight ~20 g) were purchased from Orient (Seongnam, Korea) and stored in a mouse room under specific pathogen-free conditions for 1 week before starting the experiment. All animal care and laboratory procedures were performed in accordance with the guidelines of the Animal Care and Use Committee Chonnam National University (Gwangju, Korea), National Center for Substitution, Purification and Reduction of Research Animals.

The transformed *E. coli* MG1655 [3×10^9 colony-forming unit (CFU) in 200 μ l phosphate-buffered saline (PBS)] were orally administered to mice as gavage and the intraperitoneal injection of 300 μ l of 40% L-arabinose was followed. After 1 hour, 100 μ l of 1 mg/ml biotinylated dye was intravenously injected into mice via tail vein. Mice were anesthetized with 2 % isoflurane and the fluorescence was measured by lumina S5 In Vivo Imaging System (IVIS; Perkin Elmer, MA, USA) with an excitation at 780 nm, emission at 845 nm and 1 second exposure time.

Mice were sacrificed at three hours after dye injection and *ex vivo* imaging were obtained in organs including liver and intestine. The fluorescence intensity was recorded as maximum photon flux (p/sec) over a region of interest (ROI) draw manually.

F. Bacterial counting and mSA expression

After *ex vivo* optical imaging intestine tissues were separated according to the presence of fluorescence signal. Than these tissues were gathered and weighted

based on two categories (with or without signal). These were homogenized in PBS and serially diluted with PBS. The samples were spread on LB agar plates with or without ampicillin. After overnight culture, numbers of bacterial colonies were counted and expressed as CFU/g of intestine. The number of bacteria were carried out by dividing the whole intestine or the intestine with and without signals.

To confirm mSA expression, intestines obtained from mice were homogenized in protein extraction solution [20 mM Tris-Cl (pH 6.8), 150 mM NaCl, 5 mM EDTA, 1% NP-40, and 1X Xpert protease inhibitor cocktail solution (GenDEPOT, USA)]. The homogenized tissues were sonicated (amp : 30%, pulse : 3, time : 1 min, pluse off : 15 sec) three time and centrifuged at 14,000 rpm for 30 minutes. A total of 30 µg of proteins were separated using 10% SDS-PAGE and western blot analysis was performed with specific antibodies.

G. Statistical analysis

All data are shown as mean \pm standard deviation. Two independent groups were compared using unpaired two-tailed t-tests. Comparison of multiple experimental groups was evaluated using one-way ANOVA with multiple comparisons post hoc test. A *P* value < 0.05 was considered statistically significant for all analyses. Statistical analysis was performed using GraphPad Prism 9.0 software (GraphPad, San Diego, CA, USA).

III. RESULTS

A. Plasmid engineering for mSA expression optimization

A plasmid containing the mSA gene was constructed under the control of pBAD. We introduced MBP into the mSA expression system. In addition, the expression level of mSA was improved by adding a new regulatory gene sequence of RBS (Fig. 1). First, the RBS sequence of the plasmid was analyzed to prepare a sequence library. After analyzing the TIR of the RBS-MBP-mSA plasmid using the RBS calculator program (Penn State University), a regulatory gene with a value range of the TIR from 3.97 to 42889 through the RBS Library Calculator library was built. Eight copies with good translation rates were selected and produced by attaching RBS to the N-terminus of MBP (named to pBAD-RBS-MBP-mSA). After cloning by substituting the RBS sequence of the RBS-MBP-mSA plasmid for the regulatory gene prepared according to the library, the generated colonies were selected. Eight RBS random sequences were selected from the RBS library based on translation initiation efficiency using the RBS library calculator.

B. Comparison of mSA expression and biotin binding activity

SDS-PAGE and Western blot were performed to evaluate mSA expression and biotin binding activity of the recombinant strain (Fig. 2a). When comparing mSA expression level, the expression levels of R2P-mSA(5) and R1P-mSA(9) among the eight recombinant RBS plasmid were higher than other plasmids (Fig. 2b). Four

recombinant plasmid were selected, including pBAD-mSA, pBAD-MBP-mSA (P-mSA), pBAD-RBS1-MBP-mSA (R1P-mSA), pBAD-RBS2-MBP-mSA (R2P-mSA) (Fig. 3). Next, mSA expression and biotin binding activity were compared among four kinds of recombinant strain: mSA, P-mSA, R1P-mSA, and R2P-mSA. While mSA was expressed in all strains after induction, biotin binding activities were shown in P-mSA, R1P-mSA, and R2P-mSA (Fig. 4). In particular, mSA expression and biotin binding activity were highest in R2P-mSA.

To compare the biotin binding activity among recombinant strains, a biotin uptake assay was also performed (Fig. 5). Biotinylated fluorescent dye uptake increased after L-arabinose induction in R1P-mSA and R2P-mSA. Biotin-binding activity of the recombinant strains was highest in R2P-mSA plasmid, compared to strains with the pBAD, mSA, P-mSA, or R1P-mSA strains.

C. *In vivo* imaging

Bacteria localization in mice was visualized using *in vivo* imaging system (IVIS) (Fig. 6). After oral administration of *E.coli* MG1655 with R2P-mSA to mice, L-arabinose was injected to express mSA immediately (immediate induction) or 1 h (delayed induction) after oral administration of bacteria (three mice per group). Biotinylated fluorescent dye was intravenously injected into each mouse 1 h after L-arabinose induction or bacterial administration without induction.

Compared to mice groups with dye only or without induction after bacterial administration, optical signals by biotinylated fluorescent dye were found in abdomen

in two induction groups up to 2 h after dye injection. When liver and intestinal tissues were extracted and optical signal were compared among mice groups, optical signal was found at intestinal tissues only in two induction groups. Interestingly, imaging signal was stronger in immediate induction group than in delayed induction group (Fig. 6). On the other hand, there was no significant difference of imaging signal in liver among four groups ($p=0.4112$)

D. Bacterial counts and mSA expression in liver and intestine tissues.

When the number of recombinant bacteria was investigated in liver or intestinal tissues extracted from mice with bacterial administration, the bacterial number in the intestine was similar regardless of arabinose induction (Fig. 7a). Bacteria colony was not found in liver. Among the mouse group with arabinose induction the number of recombinant strains was larger in the intestine tissues with a imaging signal than in those without imaging signal (immediate induction group: $p=0.0005$, delayed induction group: $p=0.034$, Fig. 7b). When mSA expression was assessed in intestinal tissues by Western blot analysis, mSA expression and biotin interaction were shown only in the recombinant strain with arabinose induction (Fig. 7c). Interestingly, the degree of mSA expression and biotin interaction were higher in group with immediate induction than in group with delayed induction after oral administration of bacteria.

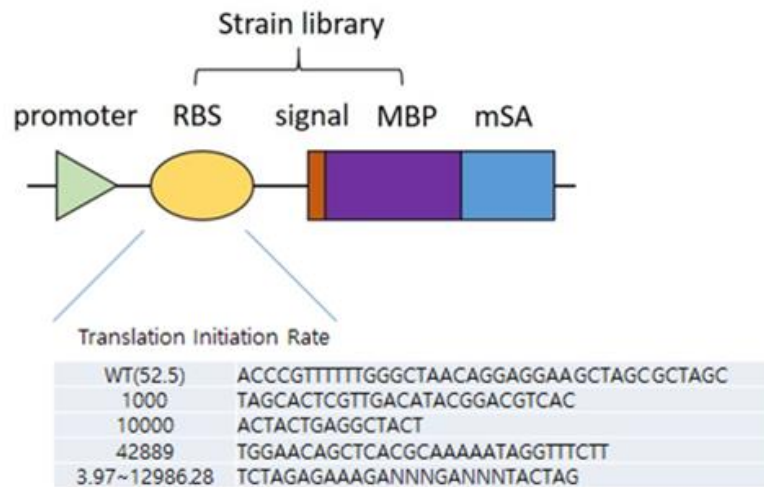


Figure 1. A schematic diagram using RBS library. After analyzing the translation initiation rate (TIR) of the RBS-MBP-mSA plasmid using the RBS calculator (Penn State University) program, a regulatory gene library having a value range of the translation initiation rate from 3.97 to 42889 was constructed through the RBS Library Calculator. After cloning the RBS sequence of the MBP-mSA (P-mSA) plasmid into the regulatory gene prepared according to the library, the resulting colonies were selected to prepare a final plasmid.

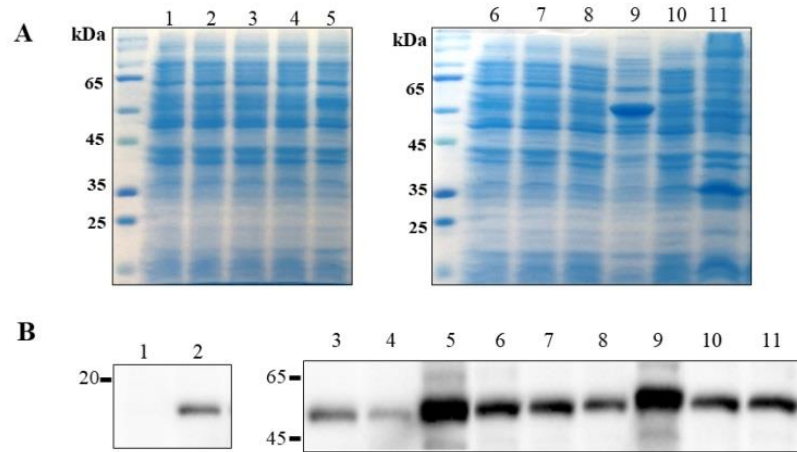


Figure 2. Confirmation of mSA expression in regulatory genes constructed according to RBS libraries. 1: pBAD, 2: mSA (15.4 kDa), 3-10 : 8 different RBS random sequence, 11: MBP-mSA (58.8 kDa). The plasmid transformed into *E.coli* MG1655 was added with 0.1% L-arabinose and incubated for three hours. (A) Results of SDS-PAGE with 12% gel (B) Result of checking the expression level of mSA using anti-His tag antibody (1:2,000)

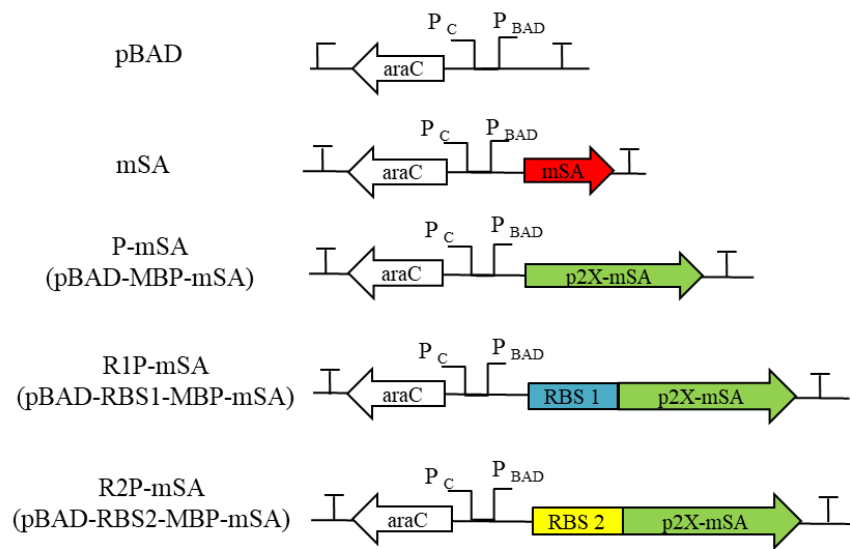


Figure 3. Engineered plasmid structure. Schematic diagram of the plasmid constructed in the pBAD promoter

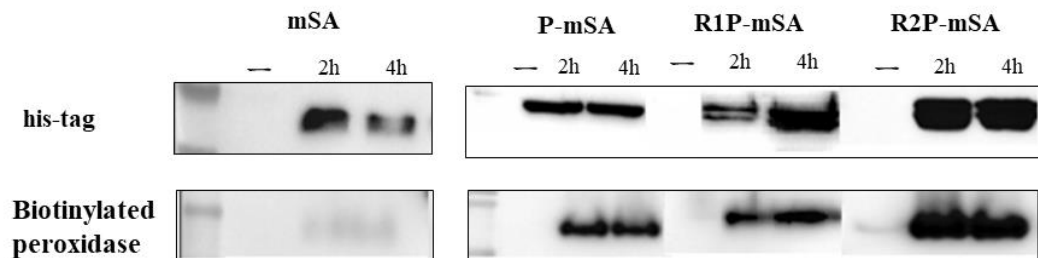


Figure 4. Evaluation of mSA expression. (Upper) mSA expression in total fractions was determined by Western blot analysis using an anti-His tag antibody (1:2,000) as primary antibody, followed by an anti-mouse IgG horseradish peroxidase as secondary antibody (1:5,000). (Lower) Functional expression of mSA was verified with a biotinylated peroxidase (1:2,000).

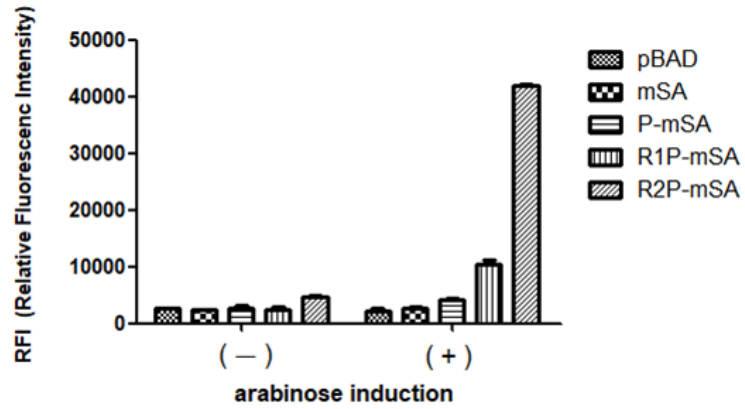


Figure 5. Biotinylated fluorescent dye uptake test. After the OD 0.5–0.7 was reached, the final concentration of 0.1% arabinose was added, and incubated for three hours, followed by additional incubation for 30 minutes by adding a biotinylated fluorescent dye. Each sample was washed at 4 OD600 and measured.

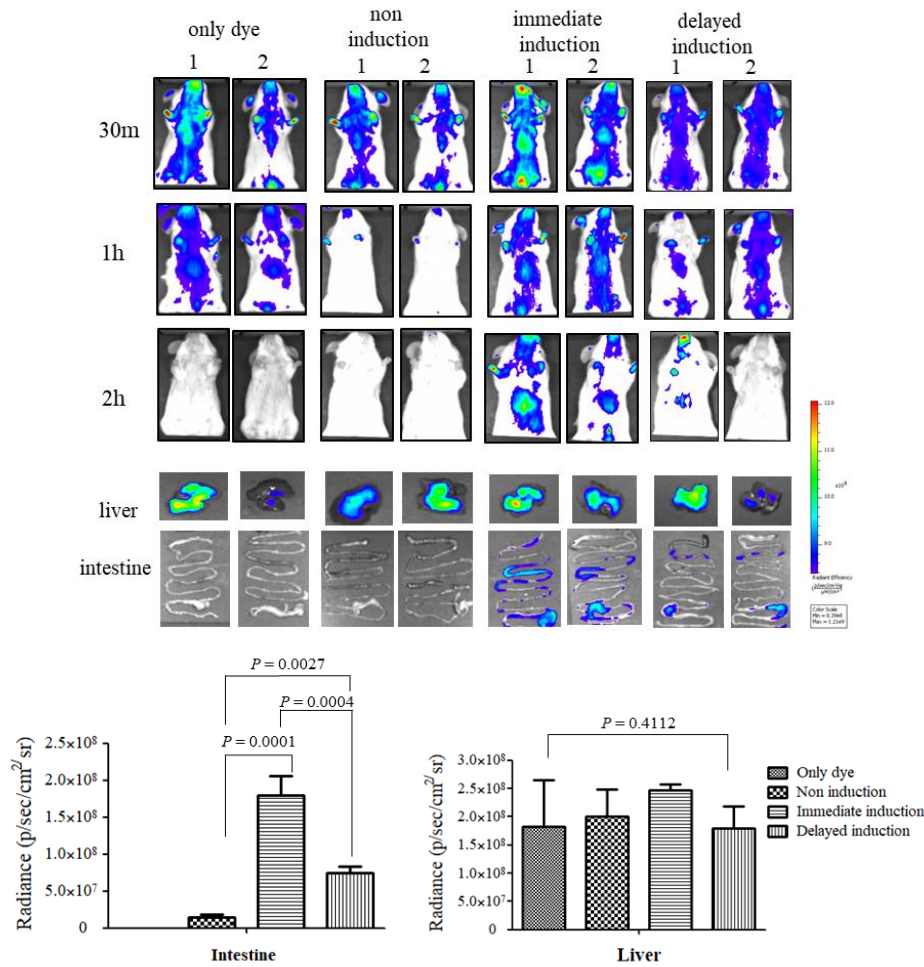


Figure 6. Optical fluorescence imaging to check bacteria tracking. L-arabinose (120 mg/300 μ l) was intraperitoneally injected immediately (immediate induction) or 1 h after (delayed induction) oral administration of *E. coli* MG1655. Then, biotinylated dye was injected intravenously into mice 1h after L-arabinose induction or without induction. Optical images were serially collected 30 min, 1h, and 2h after biotinylated dye injection. Optical signal in liver or intestine were compared among groups.

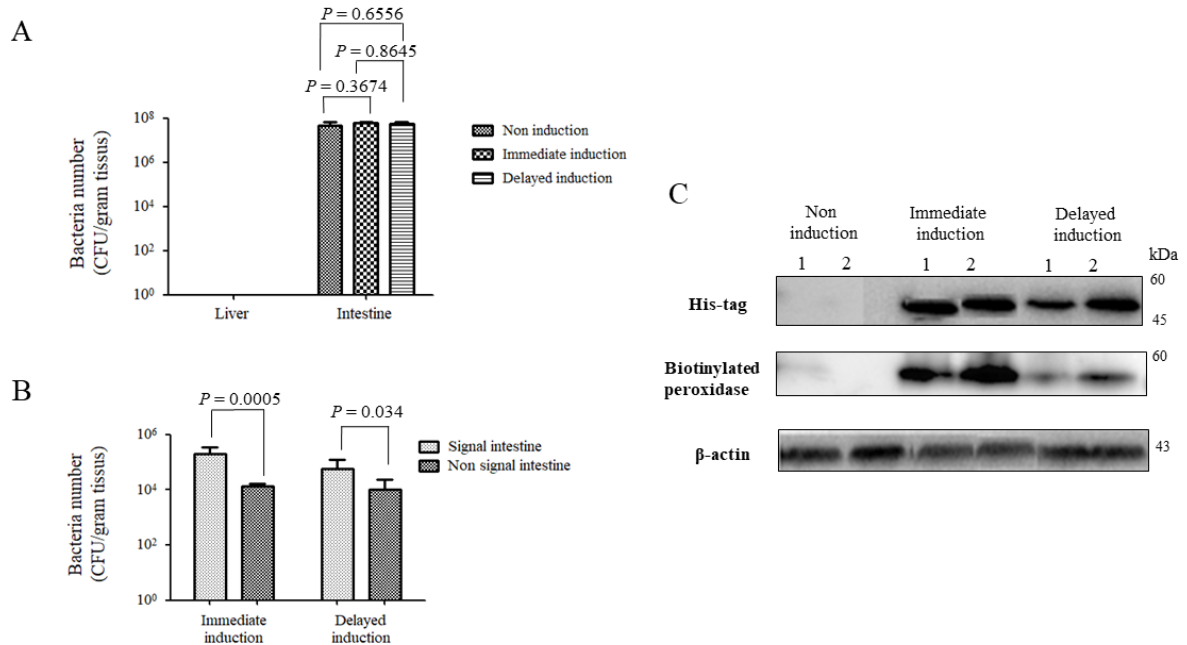


Figure 7 . Evaluation of the number of bacteria, mSA expression and biotin binding activity in mice organs. (A) Measurement of plasmid maintenance in bacteria. Bacteria were isolated on LB agar containing ampicillin from intestinal and liver tissues. (B) Colony numbers were counted after Intestinal tissue without signal and intestinal tissue with signal were separated and preceded. (C) mSA expression and biotin binding activity in intestinal tissue by Western blot analysis. Western blot was done with anti-His-tag (upper panel), biotinylated peroxidase (middle panel) and anti-beta actin antibodies (bottom panel).

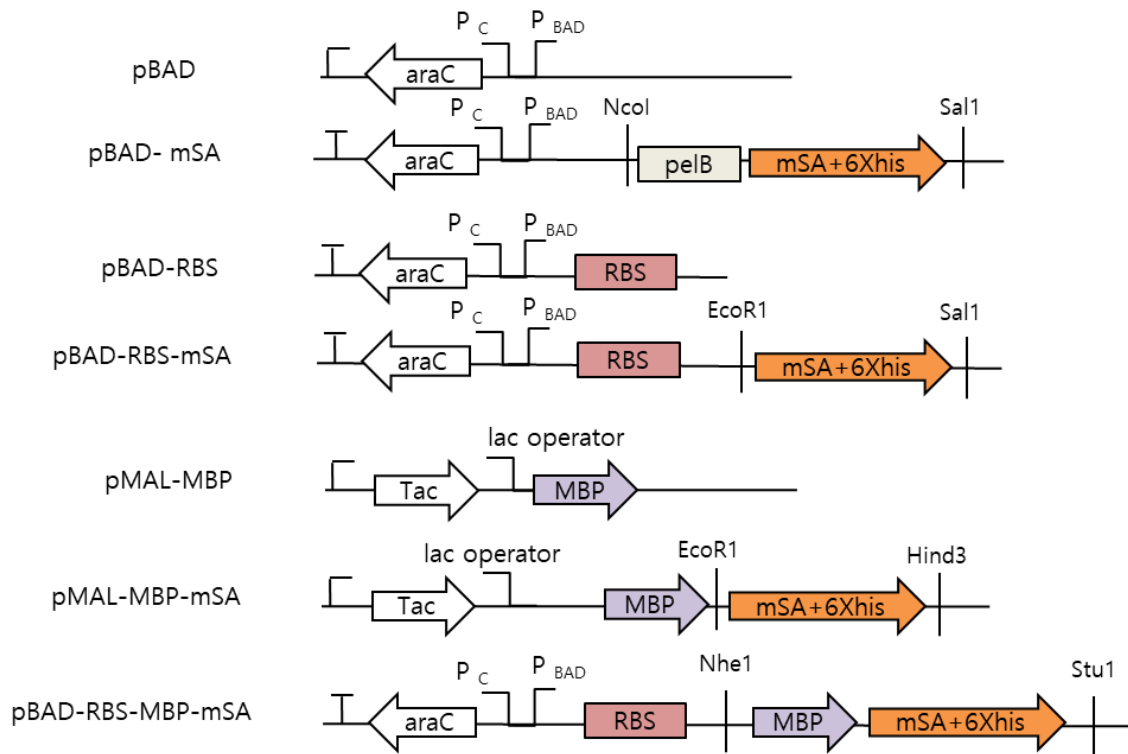


Figure S1. Construction of vectors, restriction enzymes, and plasmids used in the study. Except for pBAD-mSA, the *pelB* sequence was removed from the recombinant plasmid constructs.

Table S1. List of primer used in the study

Name	Direction	Sequence(5'->3')	Enzyme
Rhiz NcoI F	F	ATACCATGGTAAAATACCTGCTGCTGCCGACC	NcoI
Rhiz Sall R	R	ATAGTCGACTTAGGGTGGTGGTGGTGGTGTAAAC	Sall
pBAD-mSA F	F	GAATTC GCGGAAGCGGGTATCACC	EcoRI
pBAD-mSA R	R	GTCGACTTAGTGGTGGTGGTGGTG	Sall
pMAL-mSA F	F	ATA GAATTC GCGGAAGCGGGTATCACCG	EcoRI
pMAL-mSA R	R	ATA AAGCTT TTAGTGGTGGTGGTGGTGGTGTAA	HindIII
p2X-mSA F	F	ATGCTAGC ATGAAAATAAAAACAGGTGCACGC	NheI
mSA-R	R	ATGTCGAC TTAGTGGTGGTGGTGGTG	Sall

IV. DISCUSSION

In this study, it was found that when the MBP gene and the RBS gene were combined with the mSA gene, the expression of the mSA gene was enhanced improved, and biotin binding activity was significantly improved. When the bacteria were orally administered to healthy mice, the intestinal distribution of the bacteria was visualized by a biotinylated fluorescent dye that binds to streptavidin expressed in the bacteria.

The gut microbiome has many implications for many human diseases and health [13–15]. This bacterial community contains hundreds of densely populated species with compositions that change over time, from individual to individual, along the gastrointestinal tract [16, 17]. It is difficult to precisely target specific bacteria without interfering with this complex ecosystem [18]. Previously, DNA and RNA sequencing of tissue samples could only infer the composition of the gut microbiome. Although this approach can be non-invasive and yield important information for many bacterial species, but does not provide accurate information about specific type of bacteria [19, 20]. On the other hand, when performing in situ hybridization and immunofluorescence staining of microorganisms in the collected tissue to assess the information on the spatiotemporal location or density of specific microorganisms in the host animal, more spatial information can be provided, but this method is invasive in nature and difficult for real-time monitoring [18].

Several studies have been performed to visualize bacteria in vivo using

molecular imaging techniques. Bacteria could be engineered by transforming them with plasmids containing genes for bioluminescence (such as a Renilla luciferase variant (RLuc8) gene or luxCDABE operon from Photo bacterium *leioagnathi*) or fluorescent proteins [1, 2, 21-23]. Although these optical imaging systems are highly efficient for locating bacteria in vivo, there are limitations in terms of application for large animals or human because of their poor penetration of signals through tissues. On the other hand, bacteria labeled with diagnostic radionuclide had a potential for bacterial tracking in vivo to overcome penetration issues [3]. However, radionuclide-binding bacteria can be diluted after systemic circulation, which reduces in vivo imaging signal [4]. Alternatively, bacteria could be engineered to express the positron emission tomography (PET) reporter gene such as herpes simplex thymidine kinase. This strategy could phosphorylate and sequester a radiolabeled nucleoside purine or pyrimidine analog, which can be visualized by PET [24]. Instead of using an exogenous reporter gene, an endogenous thymidine kinase from the probiotic *E. coli* Nissle 1917 was used for PET imaging to phosphorylate and sequester a radiolabeled nucleoside analog although the imaging signal was very weak [4].

In our study, we developed a novel tracking system to visualize the distribution of bacteria in the body using streptavidin derivatives (mSA), a protein that is expressed in bacteria and is mainly trapped in bacteria. Streptavidin is a protein having a high binding affinity to biotin and has been applied to various biological applications by using a specific interaction with biotin [6, 8, 25, 26]. However,

conventional streptavidin has been used in tetramer or monovalent form through purification after expression in order to maintain water solubility and functionality [13, 14]. Many monomeric streptavidin-like proteins have been developed and reported in order to overcome the problem of receptor dysfunction caused by oligomerization [11, 12]. However, these proteins must also undergo purification after expression. In addition, because streptavidin-like protein is rapidly degraded in serum when injected in vivo, there is a limitation for clinical applications [27–29].

Compared to the existing monomeric streptavidin-like protein, mSA, in our study, can maintain strong binding to biotin without a separate purification process after expression. We developed a novel bacterial monitoring system that visualizes in vivo bacterial distribution with a biotinylated imaging agent that binds to expressed streptavidin.

In our study, the signal was stronger in the group induced immediately after oral administration of bacteria than in the group with delayed induction. The number of bacteria in the intestinal tissues is similar regardless of L-arabinose induction or induction interval (Fig. 7a). It has an implication that bacterial excretion from intestine might not be significant factor to affect signal intensity. Recombinant plasmid loss might not be possible because our strain included the *bom* gene. Further investigations are needed to evaluate whether the expression level of mSA may differ depending on bacterial location in the digestive tract.

Imaging system for bacterial tracking in vivo has great potential for disease managements. In a recent study, when specific intestinal microorganisms

(*Bifidobacterium pseudolongum*, *Lactobacillus johnsonii*, *Olsenella* species) were administered in combination with an immune checkpoint inhibitor, the therapeutic efficacy of the immune checkpoint inhibitor was significantly improved [30]. Our imaging-based bacterial monitoring system could be applied for determining timing of combination therapy and predicting therapeutic efficacy based on bacterial distribution. Furthermore, it is expected that our system could be applied for controlling the interaction between bacteria and host stromal cells or tissue microenvironment using biotinylated drugs as well as in vivo monitoring of beneficial microorganisms for disease management.

In conclusion, we constructed recombinant mSA to enhance the expression and solubility and developed novel bacterial tracking system by visualizing bacterial distribution in vivo using streptavidin-expressing bacteria and biotinylated optical dye. This system is expected to monitor specific microorganisms administered into the body using various biotinylated imaging agents.

REFERENCES

1. Zhao, M., et al., *Tumor-targeting bacterial therapy with amino acid auxotrophs of GFP-expressing Salmonella typhimurium*. Proc Natl Acad Sci U S A, 2005. **102**(3): p. 755-60.
2. Yu, Y.A., et al., *Visualization of tumors and metastases in live animals with bacteria and vaccinia virus encoding light-emitting proteins*. Nat Biotechnol, 2004. **22**(3): p. 313-20.
3. Quispe-Tintaya, W., et al., *Nontoxic radioactive Listeria is a highly effective therapy against metastatic pancreatic cancer*. Proceedings of the National Academy of Sciences, 2013. **110**(21): p. 8668-8673.
4. Brader, P., et al., *Escherichia coli Nissle 1917 facilitates tumor detection by positron emission tomography and optical imaging*. Clin Cancer Res, 2008. **14**(8): p. 2295-302.
5. Sano, T., et al., *Molecular engineering of streptavidin*. Ann N Y Acad Sci, 1996. **799**: p. 383-90.
6. Tran, L. and S. Park, *Highly sensitive detection of dengue biomarker using streptavidin-conjugated quantum dots*. Scientific Reports, 2021. **11**(1): p. 1-12.
7. Lim, K.H., et al., *Stable, high-affinity streptavidin monomer for protein labeling and monovalent biotin detection*. Biotechnol Bioeng, 2013. **110**(1): p. 57-67.
8. McMahon, R.J., *Avidin-biotin interactions: methods and applications*. Vol. 418. 2008: Springer Science & Business Media.
9. Zhang, D. and R. Duan, *Understanding the avidin-biotin binding based on polarized protein-specific charge*. Phys Chem Chem Phys, 2021. **23**(38): p. 21951-21958.
10. Helppolainen, S.H., et al., *Rhizavidin from Rhizobium etli: the first natural dimer in the avidin protein family*. Biochem J, 2007. **405**(3): p. 397-405.
11. Wu, S.C. and S.L. Wong, *Engineering soluble monomeric streptavidin with reversible biotin binding capability*. J Biol Chem, 2005. **280**(24): p. 23225-31.
12. Aslan, F.M., et al., *Engineering a novel, stable dimeric streptavidin with lower isoelectric point*. J Biotechnol, 2007. **128**(2): p. 213-25.
13. Gilbert, J.A., et al., *Microbiome-wide association studies link dynamic microbial consortia to disease*. Nature, 2016. **535**(7610): p. 94-103.
14. Zhou, P., et al., *Gut microbiome: New biomarkers in early screening of colorectal cancer*. J Clin Lab Anal, 2022: p. e24359.
15. Ranganathan, N. and E. Anteyi, *The Role of Dietary Fiber and Gut Microbiome Modulation in Progression of Chronic Kidney Disease*. Toxins (Basel), 2022. **14**(3).
16. Lynch, S.V. and O. Pedersen, *The Human Intestinal Microbiome in Health and Disease*. N Engl J Med, 2016. **375**(24): p. 2369-2379.

17. Crits-Christoph, A., et al., *Good microbes, bad genes? The dissemination of antimicrobial resistance in the human microbiome*. Gut Microbes, 2022. **14**(1): p. 2055944.
18. Fan, J.X., et al., *Bacteria-Mediated Tumor Therapy Utilizing Photothermally-Controlled TNF- α Expression via Oral Administration*. Nano Lett, 2018. **18**(4): p. 2373-2380.
19. Zmora, N., et al., *Taking it Personally: Personalized Utilization of the Human Microbiome in Health and Disease*. Cell Host Microbe, 2016. **19**(1): p. 12-20.
20. Hsu, B.B., et al., *In situ reprogramming of gut bacteria by oral delivery*. Nature communications, 2020. **11**(1): p. 1-11.
21. Van Zyl, W.F., S.M. Deane, and L.M.T. Dicks, *In vivo bioluminescence imaging of the spatial and temporal colonization of lactobacillus plantarum 423 and enterococcus mundtii ST4SA in the intestinal tract of mice*. BMC Microbiol, 2018. **18**(1): p. 171.
22. Daniel, C., et al., *Bioluminescence imaging study of spatial and temporal persistence of Lactobacillus plantarum and Lactococcus lactis in living mice*. Appl Environ Microbiol, 2013. **79**(4): p. 1086-94.
23. Berlec, A., et al., *In vivo imaging of Lactococcus lactis, Lactobacillus plantarum and Escherichia coli expressing infrared fluorescent protein in mice*. Microb Cell Fact, 2015. **14**: p. 181.
24. Soghomonyan, S.A., et al., *Positron emission tomography (PET) imaging of tumor-localized Salmonella expressing HSV1-TK*. Cancer Gene Ther, 2005. **12**(1): p. 101-8.
25. Boerman, O.C., et al., *Pretargeted radioimmunotherapy of cancer: progress step by step*. J Nucl Med, 2003. **44**(3): p. 400-11.
26. Udompholkul, P., et al., *Effective Tumor Targeting by EphA2-Agonist-Biotin-Streptavidin Conjugates*. Molecules, 2021. **26**(12).
27. Altves, S., H.K. Yildiz, and H.C. Vural, *Interaction of the microbiota with the human body in health and diseases*. Biosci Microbiota Food Health, 2020. **39**(2): p. 23-32.
28. Paganelli, G., et al., *In vivo labelling of biotinylated monoclonal antibodies by radioactive avidin: a strategy to increase tumor radiolocalization*. Int J Cancer Suppl, 1988. **2**: p. 121-5.
29. Xiong, X.Y., et al., *In vitro & in vivo targeting behaviors of biotinylated pluronic F127/poly (lactic acid) nanoparticles through biotin-avidin interaction*. European journal of pharmaceutical sciences, 2012. **46**(5): p. 537-544.
30. Mager, L.F., et al., *Microbiome-derived inosine modulates response to checkpoint inhibitor immunotherapy*. Science, 2020. **369**(6510): p. 1481-1489.

스트렙타아비딘 발현 박테리아를 이용한 생체 내 미생물 추적시스템 개발

임 진 희

전남대학교대학원 의과학과

(지도교수 : 권성영)

(국문초록)

본 연구에서는 박테리아에 비오틴과 강하게 결합하는 스트렙타아비딘 단백질을 발현시켜 생체 내로 투여한 박테리아의 분포를 영상용 비오틴화 약물로 시각화함으로써 박테리아의 체내 분포를 실시간으로 추적할 수 있는 새로운 형태의 박테리아 영상 추적 시스템을 개발하고자 하였다. 이를 위해 리보솜 결합 부위 (Ribosome binding site, RBS) 재조합 라이브러리에서 선택된 서열 및 말토오스 결합 단백질 (Maltose-binding protein, MBP) 단백질을 스트렙타아비딘 유전자와 융합시켜 재조합 단백질 발현량과 비오틴과의 결합력이 최적화된 *E.coli* MG1655 균주를 구축하였다. 이 재조합 플라스미드를 갖는 박테리아를 정상 마우스에 경구 투여하고 박테리아 투여 직후 및 투여 1시간 후에 각각 L-arabinose를 이용하여 스트렙타아비딘 발현을 유도하였다. 스트렙타아비딘 발현 유도 1시간 뒤에 비오틴화 형광염료를 정맥 주사하여 영상을 획득하였다.

그 결과, 형광염료만 주입하였거나 박테리아 투여 후 스트렙타아비딘 발현을 유도하지 않는 마우스 모델과 비교하여 박테리아 투여 후 스트렙타아비딘 발현을 유도한 마우스의 장에서 영상 신호가 관찰되었다. 마우스에서 장을 적출하여 신호를 비교한 결과,

스트렙타아비딘 발현 유도 마우스 군에서 영상신호가 관찰되었고, 박테리아 투여 1시간 후 스트렙타아비딘 발현을 유도한 군보다 즉시 유도한 군에서 더 강하게 관찰되었다. 재조합 균주는 스트렙타아비딘 발현 유도와 상관없이 장에 존재하였고, 재조합 균주의 수는 마우스 군 간에 특별한 차이를 보이지 않았다.

장 조직에서 웨스턴 블롯 분석을 진행한 결과 스트렙타아비딘 발현을 유도한 재조합 균주에서만 스트렙타아비딘 발현과 비오틴 결합이 관찰되었다. 이상의 결과들로 스트렙타아비딘 발현이 최적화된 재조합 박테리아와 비오틴화 형광염료를 이용하여 비침습적으로 박테리아의 체내 분포를 실시간으로 추적할 수 있는 박테리아 영상 추적 시스템을 개발하였다. 향후 다양한 형태의 비오틴화 영상제재를 이용하여 체내에 투여한 특정 미생물을 실시간 영상으로 모니터링 할 수 있을 것으로 기대된다.